

## Investigation of the Effect of Orientational Drawing on the Structural and Electroactive Properties of Vinylidene Fluoride-Tetrafluoroethylene Copolymer Films by Raman Scattering Spectroscopy

© D.K. Derimedved<sup>1,2,3</sup>, E.L. Burianskaya<sup>2,4</sup>, A.A. Maltsev<sup>2,5</sup>, I.B. Konovalova<sup>2,6</sup>, E.I. Mareev<sup>3</sup>, P.A. Mikhalev<sup>2,3</sup>, N.V. Minaev<sup>3</sup>

<sup>1</sup> National Research Nuclear University „MEPhI“, Moscow, Russia

<sup>2</sup> Bauman Moscow State Technical University, Moscow, Russia

<sup>3</sup> Institute of Photon Technologies, Crystallography and Photonics Complex, NRC „Kurchatov Institute“, Troitsk, Moscow, Russia

<sup>4</sup> National University of Science and Technology MISiS, Moscow, Russia

<sup>5</sup> Institute of Biochemical Physics, Russian Academy of Sciences, Moscow, Russia

<sup>6</sup> N.D. Zelinsky Institute of Organic Chemistry, Russian Academy of Sciences, Moscow, Russia

e-mail: drmdvdd@gmail.com

Received May 03, 2025

Revised July 25, 2025

Accepted October 24, 2025

The effect of uniaxial orientational drawing on the structural and electroactive properties of vinylidene fluoride-tetrafluoroethylene copolymer (VDF-TFE) films was investigated using Raman scattering spectroscopy (RS). Analysis of RS spectra suggests a significant increase in the fraction of the ferroactive  $\beta$ -phase upon mechanical drawing, indirectly confirmed by an increase in the piezoelectric coefficient. A correlation between structural changes and improved electrical strength of the material was established. The proposed drawing regimes and methods for analyzing the structural composition of ferroelectric polymer films can be used to create biomedical piezoelectric devices.

**Keywords:** Raman scattering spectroscopy, ferroelectric polymers, piezoelectricity, vinylidene fluoride-tetrafluoroethylene copolymer.

DOI: 10.61011/EOS.2025.11.62910.7942-25

One of the important tasks in modern medical biotechnology is the creation and implementation of compact wearable and implantable devices (sensors, power sources). Devices based on piezoceramic materials have limitations in biological environments due to low plasticity and poor biocompatibility. An alternative is provided by electroactive polymer materials, particularly ferroelectric films based on polyvinylidene fluoride (PVDF, widely known as polyvinylidene fluoride) and its copolymers [1,2]. They not only possess mechanical flexibility and biocompatibility but also have acoustic impedance close to that of water and biological tissues, which is important for implantable devices [3].

To expand application areas and improve characteristics of vinylidene fluoride-tetrafluoroethylene copolymer (VDF-TFE) films, it is necessary to study both the material itself and possibilities for its modification to enhance properties (piezoelectric, pyroelectric, mechanical).

The practical applicability of semi-crystalline polymers is determined by their structural-conformational composition, which governs electroactive properties. The crys-

talline phase of VDF copolymers is described by three macromolecular conformations:  $(TGTG^-)_n$  —  $\alpha$ -phase,  $(TTTT)_n$  —  $\beta$ -phase,  $(T3GT3G^-)_n$  —  $\gamma$ -phase [4]. The  $\beta$ -phase imparts electroactive, including piezoelectric, properties to the material; the  $\gamma$ -phase has less influence on these properties, while the  $\alpha$ -phase is electroinactive. Transitions between them can be achieved via mechanical, thermal, or electrical impacts, which is used for material modification [1]. This work examines the orientational drawing method for altering phase composition and establishes the relationship between processing conditions, structural changes, and electroactive properties [5].

For analyzing the structural composition of vinylidene fluoride copolymers, the most common methods are infrared (IR) spectroscopy and X-ray diffraction (XRD) [6]. Raman spectroscopy (RS) is also used for quantitative assessment of conformations due to the significant magnitude of the C–F-bond dipole moment and its sensitivity to molecular environment [7]. This method complements IR spectroscopy as it is sensitive to transitions inactive in IR spectroscopy [8]. In particular, more complete characterization of  $\beta$ - and

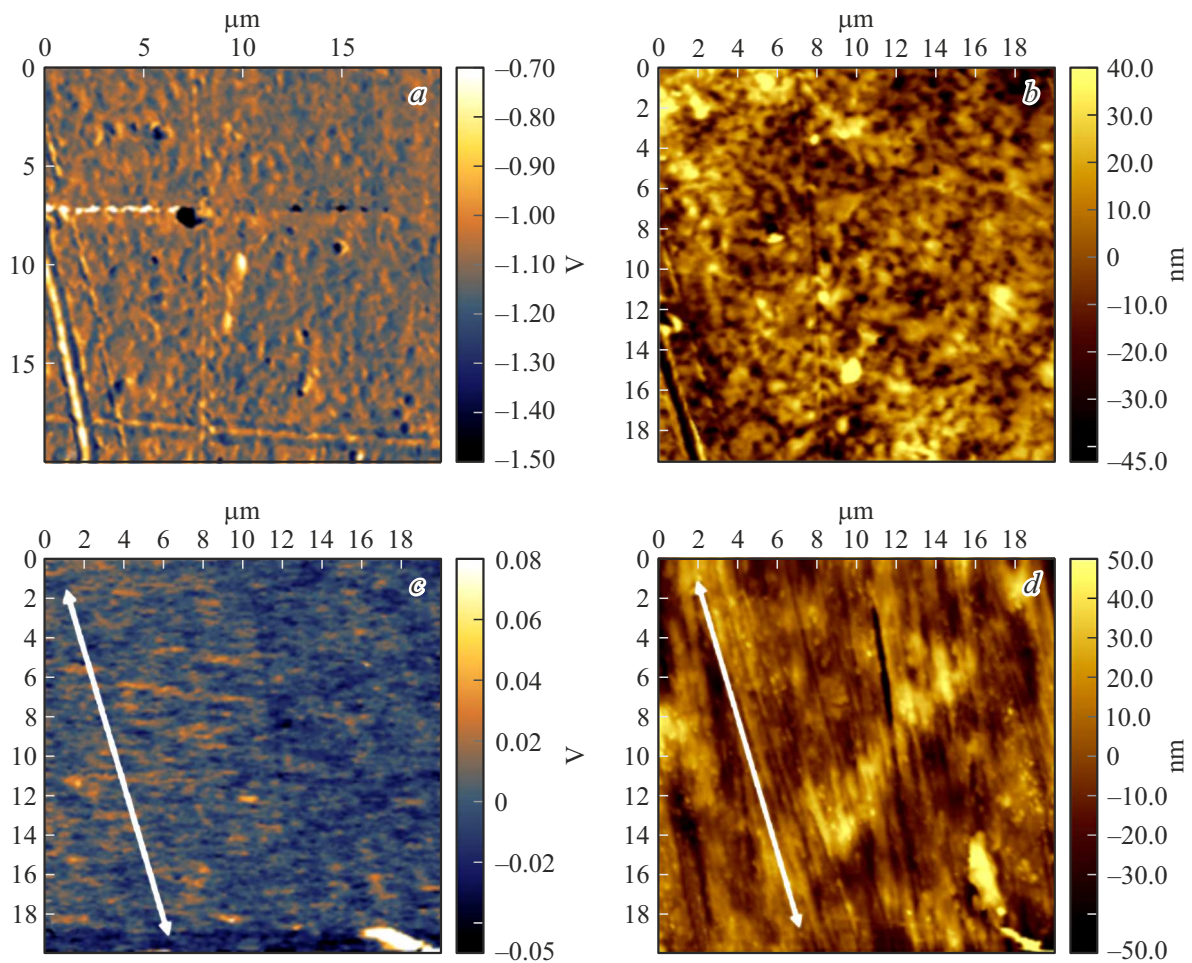


**Figure 1.** Surface potential signal distribution maps for the initial (*a*) and oriented (*c*) films and surface topography for the initial (*b*) and oriented (*d*) films; arrows on the figure indicate the drawing direction.

$\gamma$ -phases with closely spaced peaks in IR spectra is possible via RS spectrum analysis, where peaks of these conformations are separated, as performed in this work.

Within the study, two types of samples were prepared: initial isotropic and oriented VDF-TFE copolymer films in 94 : 6 ratio. Films were obtained by casting in Petri dishes from a solution of fluoroplastic F2M grade B powder (GaloPolymer, Kirovo-Chepetsk) in ethyl acetate, followed by vacuum treatment to remove residual solvent. Uniaxial orientational drawing was performed manually using a laboratory setup at 75°C with a draw ratio of  $\lambda = 4$ . The initial film sample dimensions were 20 × 20 mm with thickness 45–50 μm, after drawing, dimensions were 60 × 15 mm with thickness reduced to 30 μm.

The film samples were subjected to contact polarization on a laboratory setup [9] at room temperature for 5 min, with polarizing field strength of 200 MV/m. Considering the number of points and scatter of measured electrical strength values, the average was determined using the two-parameter Weibull model [10,11], according to which a statistical set of a large number ( $> 15$ ) of field values  $E_b$  can be described

by the function

$$F(x) = 1 - \exp \left[ -(x/\alpha)^{\beta_b} \right],$$

where  $x$  — current value of  $E_b$ ,  $\alpha$  — characteristic field at which at least 63.2% of tested samples are punctured; parameter  $\beta_b$  characterizes the dispersion of  $E_b$  relative to the mean. The studies showed an increase in electrical strength after orientation from  $E_0 = 417 \pm 7$  MV/m for the initial film to  $E_s = 468 \pm 3$  MV/m for the drawn film. This may be associated with film recrystallization during drawing and phase composition changes.

Longitudinal piezoelectric coefficients  $d_{33}$  were measured by the Berlincourt quasi-static method using an  $d_{33}$ -meter YE2730A (Sinocera Piezotronics, INC, China). For the oriented film,  $d_{33}$  was 11 pC/N, whereas for the initial film, the piezoelectric coefficient was 0.

Morphology and ferroelectric properties of the film surfaces were investigated using scanning probe microscopy (SPM, NTEGRA Prima, NT-MDT, Zelenograd, Russia). Changes in film morphology after drawing were observed (Fig. 1, *b,d*), with root-mean-square surface roughness increasing from 16 nm for the initial to 19 nm for the oriented

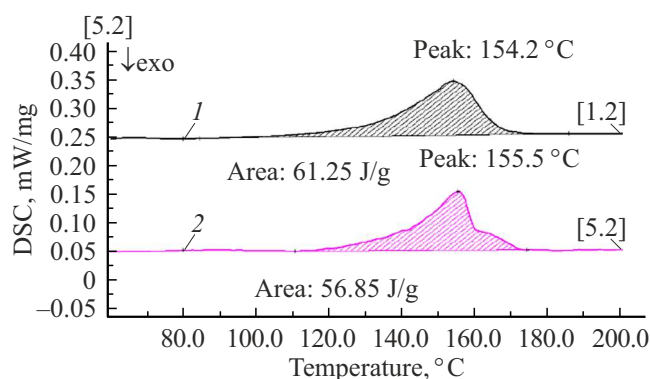


**Figure 2.** First heating DSC curves for the initial and oriented films.

film, explained by the appearance of longitudinal defects likely associated with slip bands. Kelvin probe microscopy mode yielded surface potential signal distribution maps corresponding to ferroelectric domain distributions on the film surface (Fig. 1, *a,c*). Surface potential magnitude noticeably decreases after orientational drawing, possibly due to surface defect formation. However, the obtained values differ from zero, indicating spontaneous polarization in the films.

The degree of crystallinity was determined by differential scanning calorimetry (DSC) using a NETZSCH DSC 204F1 Phoenix instrument (NETZSCH-Gerätebau GmbH) and calculated by the simplified formula

$$\chi_c = \frac{\Delta H_m}{\Delta H_m^\circ}$$

where  $\Delta H_m$  — film melting enthalpy,  $\Delta H_m^\circ$  — melting enthalpy of fully crystalline material, equal to 104.5 J/g [12]. For the initial isotropic film, it was 58%; for the oriented — 54% (Fig. 2). This indicates a slight decrease in crystallinity. Note the presence of a long low-temperature „tail“ for the isotropic sample, suggesting crystal defectiveness; thus, the drawing process likely reduced overall crystalline phase defectiveness.

RS spectra (obtained on a Thermo Nicolet Almega XR Raman spectrometer,  $\lambda = 532$  nm source,  $P_{\text{nom}} = 15$  mW, microfocus MPlan 50X objective,  $NA = 0.75$ ) were formed by averaging 20 measurements of 10 s each in the 200–3200  $\text{cm}^{-1}$  range (Fig. 3). Due to sample fluorescence, photobleaching ( $t_{\text{phb}} = 10$  min) was applied.

The relative content of each phase was determined from the ratio of spectral line intensities in the RS spectrum; the method is based on spectrum interpretation with identification of vibrational modes of chemical groups characteristic of various VDF conformations [8]. The most intense spectral lines for the three conformations are in the 800–900  $\text{cm}^{-1}$  region: 797  $\text{cm}^{-1}$  for  $\alpha$ -phase, 811  $\text{cm}^{-1}$  for  $\gamma$ -phase and 840  $\text{cm}^{-1}$  for  $\beta$ -phase and nearby low-intensity  $\gamma$ -phase peak [3]. For additional qualitative assessment, low-intensity peaks below 700  $\text{cm}^{-1}$  were also

analyzed (Fig. 4, *a*). The listed characteristic spectral line values are approximate, as they may vary depending on temperature, crystallinity, and fitting methods [8,13]. Based on these values, changes in conformational composition were analyzed. Separate analysis of TFE RS lines was not performed due to their low intensity and minor content in the study. Note a low-intensity peak at 380  $\text{cm}^{-1}$  belonging to this compound's vibrational modes. Overlap of low-intensity TFE bands on main VDF lines in the 826–829  $\text{cm}^{-1}$  region is also evident as asymmetric contour of the 839  $\text{cm}^{-1}$  line and small peaks on its slope (Fig. 4, *b*).

RS spectra of initial and oriented samples show differences in phase composition distribution (Fig. 4, *a*). For the initial VDF-TFE film, phase ratios were:  $I_\alpha : I_\gamma : I_\beta = 24 : 39 : 37$ . The low content of ferroactive  $\beta$ -phase (37%) reduces poling capability [14]. After orientational drawing, the spectral profile undergoes significant changes:  $I_\alpha : I_\gamma : I_\beta = 19 : 26 : 55$ . The increase in  $\beta$ -phase fraction to 55% indicates crystalline structure reorganization under mechanical stress. This agrees with reported recrystallization under uniaxial deformation.

It should be noted that the observed pronounced phase ratio change with characteristic spectral modifications upon mechanical drawing for VDF-TFE copolymer was obtained for the first time compared to earlier works [5].

As a result of the studies, it was established that uniaxial drawing (orientation) leads to significant structural changes in the polymer with a slight decrease in overall crystallinity and substantial crystalline structure reorganization, increasing the electroactive  $\beta$ -phase fraction from 37% to 55% (from RS spectrum analysis). Structural change data correlate well with property changes — increased electrical strength, altered surface morphology, and contact poling capability yielding piezoelectric coefficient  $d_{33}$  of 11 pC/N in the poled film.

## Funding

The work was supported by the state assignment of Bauman Moscow State Technical University (topic № FSNF-

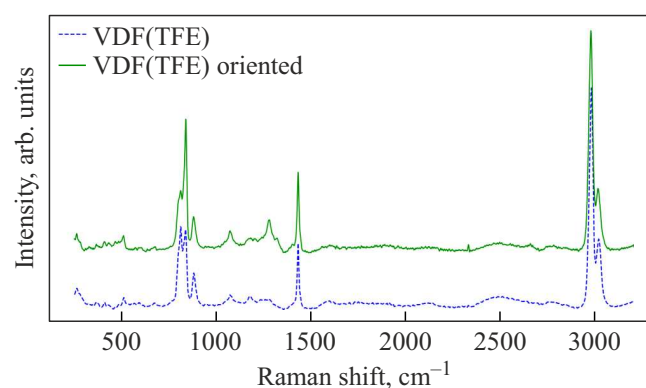


**Figure 3.** General view of RS spectra for VDF-TFE films obtained from the surface of the initial (VDF(TFE)) and oriented (VDF(TFE) oriented) samples.

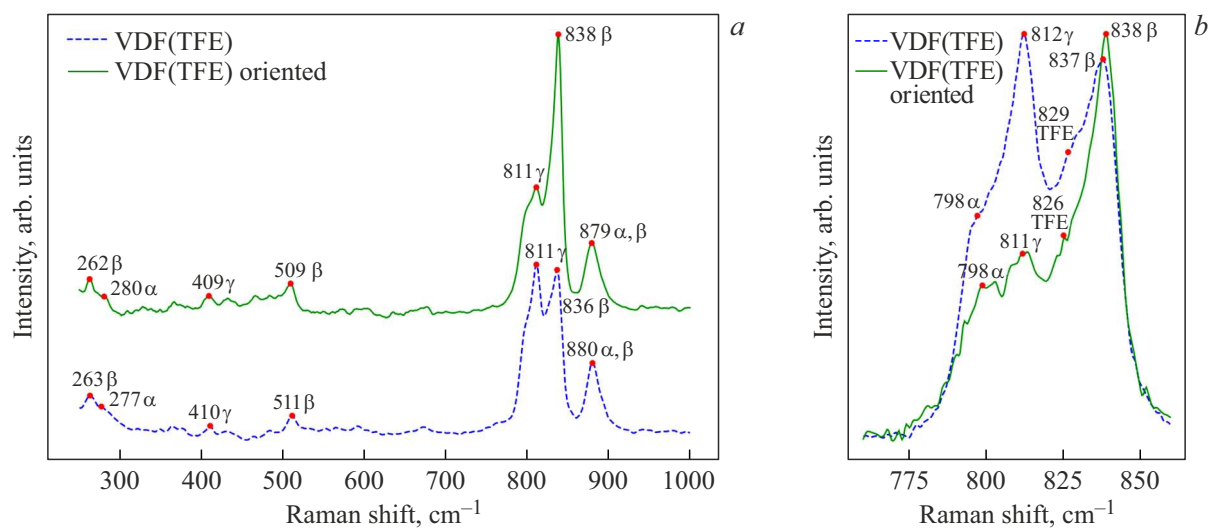


**Figure 4.** RS spectra of VDF-TFE films obtained from the surface of the initial (VDF(TFE)) and oriented (VDF(TFE) oriented) samples: (a) — studied spectral region with indicated peaks and corresponding conformations, (b) — expanded unsmoothed spectral region with pronounced peaks.

2024-0014) for developing new ferroactive polymer materials and sensor devices based on them, and by the state assignment of NRC „Kurchatov Institute“ for sample analysis by RS using equipment of the Center for Collective Use „Structural Diagnostics of Materials“ of the Crystallography and Photonics Complex, NRC „Kurchatov Institute“.

### Conflict of interest

The authors declare that they have no conflict of interest.

### References

- [1] S.K. Ghosh, D. Mandal. *J. Materials Chemistry A*, **9** (4), 1887–1909 (2021). DOI: 10.1039/D0TA08547B
- [2] P. Saxena, P. Shukla. *Polymer Bulletin*, **79** (8), 5635–5665 (2022). DOI: 10.1007/s00289-021-03790-y
- [3] V.V. Kochervinskii, M.A. Gradova, O.V. Gradov, G.A. Kirakosyan, D.A. Kiselev, M.I. Buzin, B.V. Lokshin, A.A. Korlyukov, A.A. Maltsev, I.A. Malysheva. *J. Appl. Polymer Science*, **139** (42), 1–12 (2022). DOI: 10.1002/app.53025
- [4] W. Zhang, G. Wu, H. Zeng, Z. Li, W. Wu, H. Jiang, W. Zhang, R. Wu, Y. Huang, Z. Lei. *Polymers*, **15** (13), 2766 (2023). DOI: 10.3390/polym15132766
- [5] D.K. Derimedved', V.S. Kirkin, A.A. Mal'cev, S.V. Kondrashov, E.I. Mareev, P.A. Mikhalev, N.V. Minaev. V sb.: *It Trudy XHIV Ezhegodnoj molodezhnoj konferencii s mezhdunarodnym uchastiem IBHF RAN-VUZy*, Ed. by L.V. Nedospasova, E.N. Timohina, T.Yu. Astahova, Yu.V. Tertshnoj, E.D. Nikol'skoj (RUDN, M., 2024), p. 305–308.
- [6] T.R. Venkatesan, A.A. Gulyakova, R. Gerhard. *J. Advanced Dielectrics*, **10** (5), 2050023 (2020). DOI: 10.1142/S2010135X2050023X
- [7] P.M. Resende, J.-D. Isasa, G. Hadziioannou, G. Fleury. *Macromolecules*, **56** (23), 9673–9684 (2023). DOI: 10.1021/acs.macromol.3c01700
- [8] S.M. Purushothaman, M.F. Tronco, M. Ponçot, C.S. Chitralekha, N. Guigo, M. Malfois, N. Kalarikkal, S. Thomas, I. Royaud, D. Rouxel. *ACS Appl. Polymer Materials*, **6** (14), 8291–8305 (2024). DOI: 10.1021/acspap.4c01157
- [9] S.V. Kondrashov, E.L. Burianskaya, A.S. Osipkov, V.S. Kirkin, M.V. Butina, P.A. Mikhalev, D.S. Ryzhenko, M.O. Makeev. *Int. J. Mol. Sci.*, **26** (13), 6309 (2025). DOI: 10.3390/ijms26136309
- [10] R. Tao, J. Shi, M. Rafiee, A. Akbarzadeh, D. Theriault. *Materials Advances*, **3** (12), 4851–4860 (2022). DOI: 10.1039/D2MA00072E
- [11] V.V. Kochervinskij, O.V. Gradov, M.A. Gradova. *Uspekhi khimii* **91** (11), RCR5037 (2022). (in Russian). DOI: 10.57634/RCR5037
- [12] L. Wu, Z. Jin, Y. Liu, H. Ning, X. Liu, Alamusi, N. Hu. *Nanotechnology Reviews*, **11** (1), 1386–1407 (2022). DOI: 10.1515/ntrev-2022-0082
- [13] V.I. Bachurin, N.G. Savinskij, A.P. Hramov, M.A. Smirnova, R.V. Selyukov. *Poverkhnost'. Rentgenovskie, sinhrotronnye i nejtronnye issledovaniya*, **11**, 58–68 (2024). (in Russian) DOI: 10.31857/S1028096024110075
- [14] E. Burianskaya, S. Kondrashov, A. Osipkov, S. Lermontov, N. Vlasenko, D. Derimedved, T. Petrova, M. Makeev, D. Kiselev. In: *2024 8th International Conference on Information, Control, and Communication Technologies* (IEEE, Vladikavkaz, 2024), p. 1–4. DOI: 10.1109/ICCT62929.2024.10874917

Translated by J.Savelyeva